Boundary-Layer Meteorol (2014) 150:185–214
DOI 10.1007/s10546-013-9862-6

ARTICLE

Modelling of the Thermodynamical Diurnal Cycle in the Lower Atmosphere: A Joint Evaluation of Four Contrasted Regimes in the Tropics Over Land

F. Couvreux · F. Guichard · A. Gounou · D. Bouniol · P. Peyrillé · M. Köhler

Received: 20 November 2012 / Accepted: 12 August 2013 / Published online: 8 October 2013

Abstract The diurnal cycle is an important mode of variability in the Tropics that is not correctly predicted by numerical weather prediction models. The African Monsoon Multidisciplinary Analyses program provided for the first time a large dataset to document the diurnal cycle over West Africa. In order to assess the processes and mechanisms that are crucial for the representation of the diurnal cycle, four different regimes that characterize the varying conditions encountered over land along a surface-temperature gradient are selected. A single-column modelling framework is used in order to relate the features of the simulated diurnal cycle to physical processes in these four distinct cases. Particular attention is given to providing realistic initial and boundary conditions at the surface and in the atmosphere, enabling the use of independent data for the evaluation of the simulations. The study focuses on the simulation of the surface energy budget and low-level characteristics and analyzes the balance between cloud/surface/boundary-layer processes at the sub-diurnal time scale. The biases and drawbacks of the simulations are found to change along the temperature gradient but they always involve the representation of clouds. They also explain parts of the bias obtained with the same model when used in a less constrained configuration. Surface–atmosphere–cloud interactions arising at the sub-diurnal time scale are invoked to explain the distinct features of the low-level diurnal cycle observed over West Africa.

Keywords African Monsoon Multidisciplinary Analysis campaign · Diurnal cycle · Single-column model · Surface–atmosphere–cloud interactions

1 Introduction

The diurnal cycle is a dominant mode of variability in the Tropics (Hastenrath 1995) but its accurate representation in numerical models is not yet reached. The representation of

F. Couvreux (✉) · F. Guichard · A. Gounou · D. Bouniol · P. Peyrillé
CNRM-GAME, Météo-France & CNRS, Toulouse, France
e-mail: fleur.couvreux@meteo.fr

M. Köhler
Deutscher Wetterdienst (DWD), Frankfurter Str.135, 63067 offenbach, Germany

the diurnal cycle of precipitation (Yang and Slingo 2001; Betts and Jakob 2002a; Dai and Trenberth 2004; Nikulin et al. 2012; Roehrig et al. 2013) is still a challenge for global and regional models, which tend to simulate the maximum of precipitation a few hours too early, too much in phase with the maximum insolation. This issue is particularly important over land where the amplitude of the diurnal cycle is large (Dai 2001; Nesbitt and Zipser 2003; Medeiros et al. 2005). A number of studies highlighted the role of parametrizations in shaping the simulated diurnal cycle of convection (Betts and Jakob 2002a; Guichard et al. 2004); these studies underline an absence or a poor representation of the growing cumulus phase. Progress on the physics of convective parametrizations appears to correct at least partially this drawback (Rio et al. 2009; Genio and Wu 2010; Stratton and Stirling 2012; Rio et al. 2013). However the representation of the diurnal cycle remains an important issue for numerical models, under convective cloudy as well as clear-sky conditions (Svensson et al. 2011). Furthermore, because of its large amplitude, coherent phase and short time scale, testing its representation in numerical models appears an attractive methodology for evaluating model physics (Dai and Trenberth 2004).

Betts and Jakob (2002b) showed that several major global model deficiencies are reproduced when using a single-column model (SCM), in particular the diurnal error signature. This type of model allows an independent evaluation of the model physics mainly active in the vertical at global circulation model gridscale (on the order of a few tens of kilometres) with respect to large-scale circulation (on the order of hundreds of kilometres) involving mainly the representation of the dynamics of the atmospheric flow. Other studies used simplified models to evaluate model physics; for example, Santanello et al. (2007) used a surface–atmosphere coupled SCM and observations from the Atmospheric Radiation Measurement Southern Great Plains site to examine land–atmosphere coupling and its control on atmospheric boundary-layer (ABL) development. They showed that atmospheric stability and the soil moisture are key variables for boundary-layer growth. Schlemmer et al. (2011) used an idealized cloud resolving model coupled to a land-surface model to analyze the sensitivity of the diurnal cycle of convection to different initial temperature and moisture atmospheric profiles and soil moisture conditions. They indicated that in the model equilibrium, the prescribed stability was important while the initial profile of humidity had a negligible impact because, at equilibrium, the moisture was mainly controlled by convection. However, this conclusion is probably sensitive to the atmospheric profiles used for relaxation as well as the soil properties. Here we propose to use a SCM to analyze the representation of the diurnal cycle and to determine the main involved processes.

The diurnal cycle over West Africa has only recently been presented and studied as such (Parker et al. 2005; Lothon et al. 2008; Gounou et al. 2012). Over land in general, and thus over West Africa, the diurnal cycle of precipitation is poorly simulated in global and regional models (Nikulin et al. 2012; Rio et al. 2013; Roehrig et al. 2013). Peyrillé and Lafore (2007) compared the diurnal cycles in the Inter-Tropical Convergence Zone (ITCZ) and the Saharan depression in numerical simulations but lacked observations to corroborate their results. Parker et al. (2005) used observations to show that an acceleration of the monsoon flow occurs at night whereas, during the day, the boundary-layer development inhibits the northward propagation of this flow. A major interest of the field campaign of the African Monsoon Multidisciplinary Analyses (AMMA) program (Redelsperger et al. 2006) was the collection of a large dataset characterizing the diurnal cycle at low levels in West Africa, in particular through an intensification of the radiosounding frequency (Parker et al. 2008). Gounou et al. (2012, G12 in the following) analyzed radiosoundings, surface meteorological, radiative and turbulent flux measurements and ceilometer data collected at four sites (Cotonou, Parakou, Niamey and Agadez, see Fig. 1 of G12) during two periods of 10 days, one before the

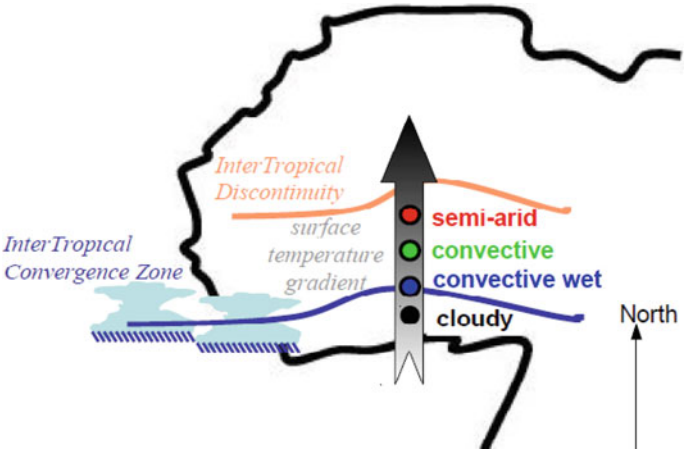

Fig. 1 Schematic of the different types used in this study. The four types are localized along a meridional surface temperature gradient (with temperature increasing towards the north) at a varying distance from the InterTropical Dis-continuity that marks the limit between the moist air advected from the south and the dry air advected from the north

monsoon onset (20–29 June 2006) and one during the core of the monsoon (1–10 August 2006). The authors showed how the diurnal cycle at low levels varies with latitude and also the season (before or during the monsoon). In particular, they identified four different regimes that cover a large range of the observed diurnal-cycle variety; they are used here as a test-bed for model evaluation. Those four regimes are well organized along a low-level temperature gradient as illustrated in Fig. 1. The cloudy type is weakly precipitating and relatively cool and moist. The convective wet type is also moist and heavily precipitating (it is typical of the conditions observed in the core of the ITCZ). The convective type is warmer and precipitating (it is typical of the full monsoon within the northern branch of the ITCZ). The semi-arid type is hot and typical of semi-arid conditions encountered in the Sahel prior to the monsoon. These findings are broadly consistent with recent studies of the annual cycle in the Sahel. For instance, the diurnal cycle of surface thermodynamics and radiative fluxes explored by Guichard et al. (2009) using data collected over the central Sahel displayed variations through the year that involve strong couplings of thermodynamics and radiative parameters.

The diurnal cycle of clouds has also been recently investigated over this region. Bouniol et al. (2012) showed, using observations from the atmospheric radiation measurement mobile facility deployed in Niamey, Niger in 2006, that both low, mid, high and convective clouds displayed a strong diurnal cycle. Knippertz et al. (2011) also showed that low clouds over the southern West Africa peak at night and in the early morning, due to the ABL diurnal cycle and the development of the nocturnal low-level jet, leading to the predominance of fully overcast nights that are hardly predicted by climate models.

A major motivation of this study is the general need to improve the representation of the diurnal cycle in models. The goals of the current study are, (i) to investigate the ability of a research numerical model to represent the distinct diurnal cycle types of the atmospheric low levels observed in West Africa, and (ii) to analyze the simulated balances between cloud, surface and boundary-layer processes at the diurnal time scale and how they differ from observations. In particular, we seek to determine whether model errors are similar or not for the different cases. A specific modelling framework is developed taking advantage of the numerous observations collected during the AMMA field campaign. The model is used in

a single-column configuration with a full set of parametrizations including a land-surface model, boundary-layer turbulence, shallow and deep convection and radiation schemes. The paper is organized as follows: Sect. 2 presents an evaluation of numerical weather prediction (NWP) model skills over the given cases as a motivation to investigate the representation of the atmospheric low levels. Section 3 describes the proposed framework detailing the model, the initial conditions and large-scale forcing, the different simulations as well as the observations used for evaluation. Section 4 presents the simulation results and discusses the balance between cloud, turbulent and radiative processes, while Sect. 5 presents sensitivity results to the large-scale advection, the land–atmosphere coupling and the presence of the diurnal cycle. The paper ends with conclusions and perspectives.

2 Evaluation of NWP Models

In order to highlight some difficulties in the use of NWP models to represent the different diurnal cycles encountered over West Africa, we evaluate the characteristics of the low levels simulated in two NWP models for the four cases. For this purpose, the 3-h frequency radiosounding observations collected during AMMA are used. The simulations consist of 24-h forecast runs initiated every day at 0000 UTC from an analysis.

2.1 The Forecast Models

The two forecast models shown here are: the European Centre for Medium-Range Weather Forecasts (ECMWF) model (Agusti-Panareda et al. 2010) and the Global French model (Karbou et al. 2010). The ECMWF model (cycle 32) was run with a horizontal resolution of about 40 km and 91 vertical levels. All observations available at the highest resolution were assimilated to perform the analyses, in particular soundings. These are not the common operational runs that are evaluated here but special simulations corresponding to the ECMWF AMMA reanalyses (Agusti-Panareda et al. 2010). Note that, in the following, the profiles from this reanalysis are used to derive initial conditions and large-scale advection for the SCM simulations. The second model is the Météo-France assimilation and forecast system (Action de Recherche Petite Echelle Grande Echelle, ARPEGE), and also assimilated additional data as described in Karbou et al. (2010). Runs were performed with a horizontal resolution of about 25 km and 61 vertical levels. Vertical profiles of the thermodynamic and dynamic variables are extracted at the closest model grid point for both models for each type. The first 24 h of the forecast are evaluated.

2.2 Results

G12 already showed evaluations of NWP model representation of the diurnal dynamics for the semi-arid case with poor representation of the fine structure observed at nighttime. Here we focus on the representation of the diurnal thermodynamics for all four types by comparing the diurnal cycle of different variables in the observations and NWP predictions for the same 10-day periods. Both NWP models are able to distinguish the four cases and reproduce broadly the differences between them besides some biases as shown in Fig. 2. Note that Agusti-Panareda et al. (2009, 2010) and Karbou et al. (2010) emphasize the impact of thermodynamical biases in current NWP forecasts on the boundary layer, precipitation and large-scale circulations (e.g. Fig. 17 of Agusti-Panareda et al. (2009), or Fig. 17 of Karbou et al. (2010)). Even after substantial improvements of the analyses (via a more

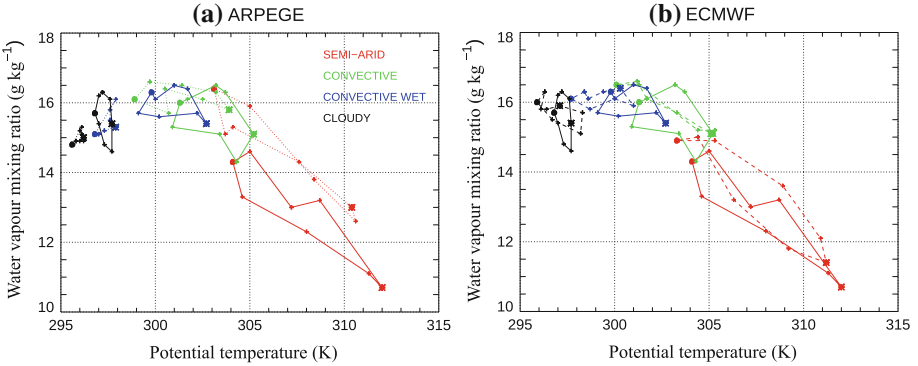

Fig. 2 Diurnal cycle of r_v and θ in the 500 m lower levels for the four types in observations (*full line*) and **a** ARPEGE (*dotted line*) and **b** ECMWF (*dashed line*). The *dots* corresponds to the values at 0600 and the stars at 1800 UTC

careful assimilation of data or the assimilation of additional data), these studies underlined the rapid development of biases in the forecast that they attributed to the parametrizations of physical processes. Both NWP models have difficulties in representing the cloudy type. This type is characterized by a diurnal cycle in the water vapour mixing ratio (r_v) but weak changes in potential temperature (θ) whereas both models predict a significant diurnal cycle in both θ and r_v.

In more detail, ARPEGE tends to be too cold (1–2 K) for all cases (especially for the convective wet type, blue line), too moist (0.5–1 g kg^{-1}) in the dry cases and too dry (0.5 g kg^{-1}) in the moist cases. All types, except semi-arid have a too small (large) r_v (wind speed) diurnal cycles. The amplitude of the diurnal cycle of θ is underestimated in the convective wet type (blue line). The maximum cooling (as well as the maximum nocturnal jet when present, but not shown) tends to occur too early. Generally, the ARPEGE model underestimates the boundary-layer development in semi-arid and convective types leading to a too small boundary-layer height (which is consistent with the θ and r_v bias).

The ECMWF analysis behaves slightly better both for the dynamic (not shown) and thermodynamic components. Nevertheless, there is a cold bias (1 K) for the moist cases, an underestimation of the amplitude of the diurnal cycle of specific humidity for all cases except the semi-arid one and an overestimation of the amplitude of the θ diurnal cycle for the cloudy type. The model has difficulties in reproducing the morning moistening (observed for all cases except for the semi-arid). The ABL warms and grows too quickly in the morning. The ABL height tends to be too high especially for the semi-arid type, consistent with Agusti-Panareda et al. (2010). In addition, this model is not able to reproduce the weakly stratified nighttime boundary layer observed in the semi-arid type (G12).

The evaluated runs started at 0000 UTC and the conclusion might be slightly different for runs starting at 1200 UTC. Nevertheless, smaller but qualitatively similar errors exist in the model analysis (not shown) suggesting that the present results do not change much with change in lead-time.

The errors in dynamics occur mainly at nighttime whereas errors in thermodynamics grow during daytime, thus emphasizing the importance of analyzing the diurnal cycle. This section suggests that there are still some weaknesses in the diurnal cycle of the processes operating at low atmospheric levels in current NWP models. The following section proposes a modelling

framework that allows us to tackle the different sources of errors of the diurnal cycle of θ and r_v at low levels.

3 The Proposed Framework

The proposed methodology involves the use of a SCM fed by the best estimates of the initial conditions as well as the large-scale advection. Both are extracted from the specific re-analysis forecasts carried out for the AMMA field campaign (which incorporates an unprecedented amount of data over the region—Agusti-Panareda et al. 2010). The ECMWF re-analysis forecasts have been evaluated in the previous section and shown to be slightly better in reproducing the diurnal cycle of the low levels than ARPEGE. The determination of realistic advection fields is an important issue. Here, we use the advection fields of the ECMWF AMMA re-analysis, because, to our knowledge, it provides the best available advection dataset for our purpose. Note that the realism of the synoptic fluctuations in the advection terms has been evaluated (not shown). Previous studies have used mixed-layer models to investigate the observed behaviour above the Sahel, such as Goutorbe et al. (1997) and Van Heerwaarden et al. (2010) but were limited to the daytime boundary layer. Couvreux et al. (2009) or Braam and Vila-Guerau de Arellano (2011) proposed an intermediate complexity modelling framework in order to tackle the origin of mesoscale boundary-layer heterogeneities or the role of surface heterogeneities. The present framework represents a trade-off between idealized single-column models (Santanello et al. 2007 for example) and full 3D model simulations. The use of a SCM configuration allows us to investigate the representation of the physical processes through the parametrizations within a realistic large-scale context (Betts and Jakob 2002a, b). This configuration is used here in order to investigate the coupling between the surface, atmosphere and clouds over land at diurnal and synoptic time scales in the continental Tropics.

3.1 The Mesoscale Research Model Meso-NH

The modelling framework is derived from a specific use of the Meso-NH model whose dynamical part is described in Lafore et al. (1998). A turbulence parametrization based on a prognostic equation of the turbulent kinetic energy (1.5-order closure scheme, Cuxart et al. 2000) and a mass-flux scheme are activated in order to represent thermals (Pergaud et al. 2009). The surface energy exchanges are represented according to four possible surface-type patches (natural land surfaces, urban areas, ocean, lake) included in a grid mesh. The interactions between soil, biosphere and atmosphere (ISBA) scheme (Noilhan and Planton 1989) is used for the natural land surfaces, and predicts prognostically surface fluxes and soil temperature and moisture at two levels. The radiative scheme is basically the same model as in the ECMWF model and includes the rapid radiative transfer model (RRTM) parametrization (Mlawer et al. 1997) for longwave radiation. The effects of aerosols on radiation are taken into account, using the climatological distribution of Tegen et al. (1997). The convection scheme is described in Bechtold et al. (2001). The microphysical scheme includes the three water phases with five species of precipitating and non-precipitating liquid and ice water (Pinty and Jabouille 1998). In this study, the model is run in a single-column version with 97 vertical levels: the first level is 20 m thick and the levels above are thinner than 100 m up to 5,000 m. The model top is at 20 km with an absorbing layer in the upper 2.5 km.

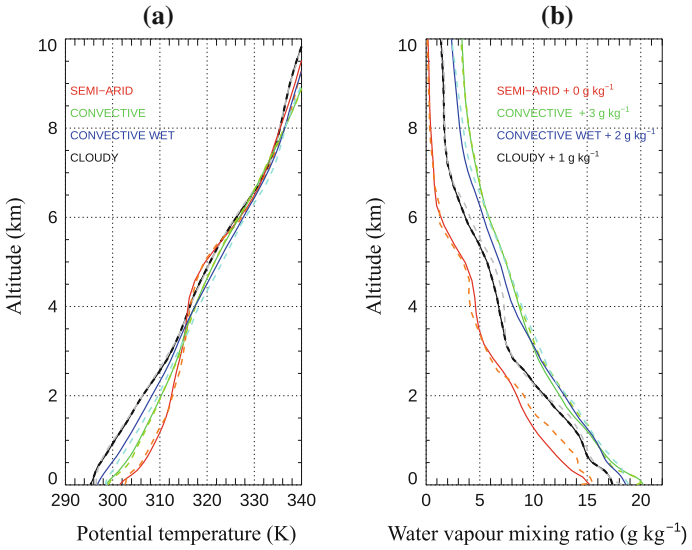

Fig. 3 0600 UTC mean vertical profile of **a** potential temperature and **b** water vapour mixing ratio from ECMWF AMMA reanalysis (*full line*) and from radiosoundings (*dashed line*) averaged over the 10-day period for the four types (see legend). The following increments have been added in order to separate the water vapour mixing ratio profiles (zero for semi-arid, 1 g kg^{-1} for cloudy, 2 g kg^{-1} for convective wet and 3 g kg^{-1} for convective)

3.2 Initial and Boundary Conditions

Vertical profiles from the ECMWF AMMA re-analysis (Agusti-Panareda et al. 2010) at 0600 UTC at the closest model grid-point are used as initial conditions. They are interpolated at the SCM vertical grid (finer than the ECMWF AMMA re-analysis up to 8 km). Figure 3 presents the 10-day averaged profiles of θ and r_v for the different cases. The sounding measurements are overplotted (dotted lines). Both profiles are similar. Note the modification from stable conditions for the cloudy type (black line, with a lapse rate of about 0.005 K m^{-1}) to less and less stable conditions for convective wet, convective and semi-arid types respectively. The former presents a layer with a small lapse rate (0.002 K m^{-1}) between 1 and 4.5 km corresponding to the Saharan air layer (Parker et al. 2005). Concerning the r_v profiles, only the semi-arid type (red line) has a distinct profile with drier conditions. Those initial profiles have the advantage to be smoother compared to radiosoundings and to be consistent with the prescribed large-scale advection.

Soil properties and vegetation cover used to initialize the simulations come from the Ecoclimap database (Masson et al. 2003) and surface properties (soil moisture and temperature) are extracted from the AMMA land-surface model intercomparison project (Boone et al. 2009). These data are described in Table 1.

The total advection is also extracted from the AMMA re-analysis for each day and each case using an area roughly 40 km $\times$ 40 km wide around each site. The composite 10-day average diurnal cycle of total advection (vertical plus horizontal components) of θ and r_v for the different cases is shown in Fig. 4. For the semi-arid type, the total advection mainly affects the low levels of the atmosphere with, in particular, a nighttime moistening (0.7 g kg^{-1} h^{-1}) and cooling (-0.8 K h^{-1}) due to the acceleration of the monsoon flow

Table 1 Surface initialization for the different cases: soil characteristics, surface and soil temperature and moisture, cover types

	Semi-arid	Convective	Convective wet	Cloudy
% clay	7	7	19	17
% sand	79	79	43	51
Surface temperature (K)	297.6	296.1	294.8	296.3
Ground soil temperature (K)	300.2	300.1	300.	300.
Surface soil moisture	0.044	0.204	0.264	0.183
Ground soil moisture	0.028	0.122	0.220	0.216
Covers	Semi-arid open shrublands (86 %), semi-arid closed shrublands (7 %), bare land (5 %), inland water (2 %)	Semi-arid open shrublands (86 %), semi-arid closed shrublands (7 %), bare land (5 %), inland water (2 %)	Tropical wet grassland (40 %), tropical crops (40 %), wetland (10 %), tropical open shrublands (10 %)	Tropical crops (35 %), tropical open shrublands (35 %), sea (15 %), inland water (5 %), wetlands (5 %), tropical grassland (5 %)

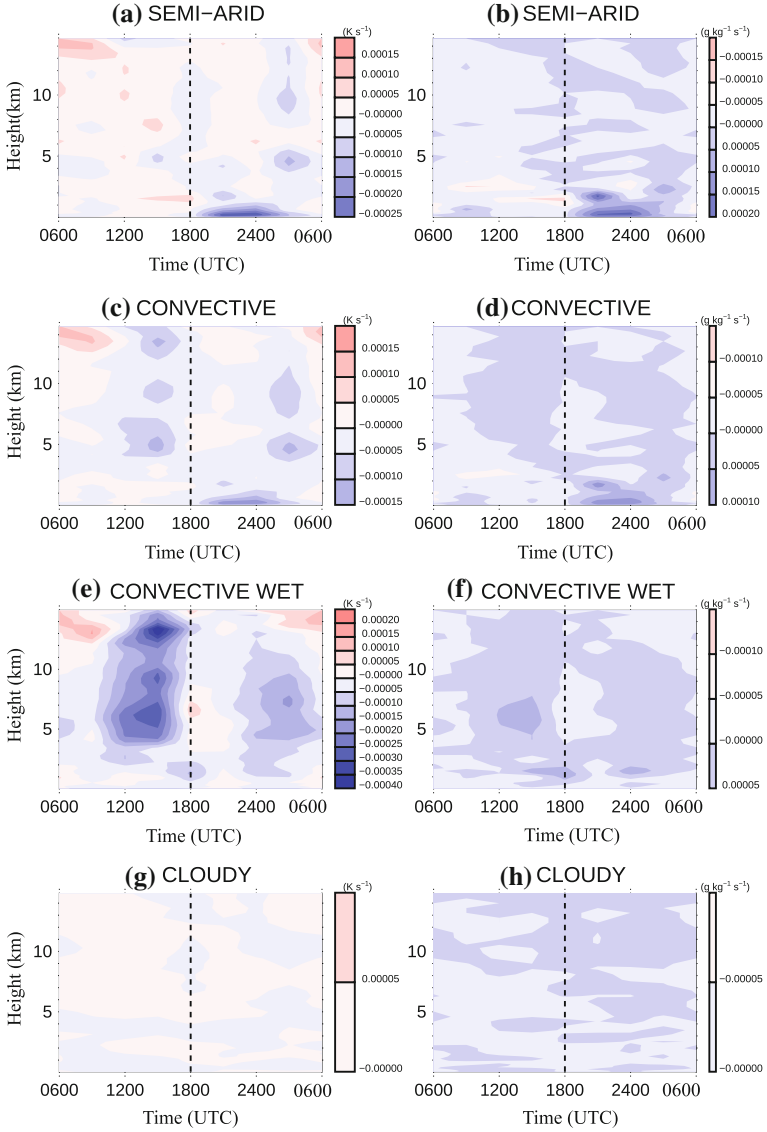

Fig. 4 Diurnal composite of potential temperature (in K s^{-1}, *left figures*) and water vapour mixing ratio (in g kg^{-1} s^{-1}, *right figures*) large-scale advection derived from the AMMA ECMWF reanalysis for the different types. The *dashed vertical line* separates the day and night

by the low-level jet (Lothon et al. 2008) and a daytime warming and drying up to 5,000 m associated with the elevated return flow from the north-east. This is mainly horizontal advection at least for the low levels (not shown). For the convective type, a similar but weaker low-level pattern is present linked to the advection by the nocturnal low-level jet as well as a moistening/cooling in the early morning and the early afternoon in the upper levels linked to deep convection and associated mainly with vertical advection. Note that a small correction (of about 10 %, similar to Guichard et al. 2000) was applied to the advection here in order to

Table 2 Summary of the set-up of the different simulations

Name of the simulation	Advection	Surface fluxes	Radiation	Reinitialized every day
REF	Synoptic	Interactive	Interactive	Yes
COMPO	Diurnal composite advection	Interactive	Interactive	No
CST	Diurnal averaged composite advection	Interactive	Interactive	No
FLUX	Diurnal composite advection	Prescribed: diurnal composite of surface fluxes from REF	Prescribed: diurnal composite of radiative tendency from REF	No

avoid the development of non-physical biases in the long duration simulation. For the convective wet type, the dominant advection (cooling, $-0.9\,\mathrm{K\,h^{-1}}$ and moistening, $0.2\,\mathrm{g\,kg^{-1}\,h^{-1}}$) is present in the mid-troposphere and is identified as vertical advection with a semi-diurnal cycle maximized in the early afternoon and early morning, a timing that is tightly linked to the moist convection simulated in the re-analysis. Note that this corresponds to a somewhat too early onset of convection (Bechtold et al. 2004);the sensitivity to this diurnal timing is addressed in Sect. 5. However, at the daily time scale, the large-scale vertical velocity is consistent with the observed precipitation and brightness temperature, indicating that the synoptic variability of the occurrence of deep convection is well reproduced by the AMMA re-analysis (not shown). The cloudy type is characterized by relatively weak advection with moist and cold advection in the lowest 500 m during the day linked to sea-breeze circulations, and dry and warm advection between 1 and 3 km heights.

In all the simulations, the vertical profiles of wind are nudged towards the re-analysis profiles with a constant damping time of 3 h.

3.3 The Simulations

Different simulations, presented in Table 2, are run for each case:

i a 10-day simulation, referred to as REF, using synoptically varying large-scale advection (see details above) and reinitialized every day at 0600 UTC
ii a 10-day simulation, referred to as COMP, (without reinitialization) that uses a diurnal composite of advection presented in Fig. 4 in order to identify the role of synoptically varying large-scale advection as well as some biases that can develop in a longer duration simulation. There is no synoptic variability of advection in the simulation.
iii a 10-day simulation, referred to as CST, with constant profiles of advection, obtained from diurnally-averaging the advection used in COMP, in order to assess the role of the diurnal cycle of the large-scale advection
iv a 10-day simulation, referred to as FLUX, using COMP advection with prescribed diurnal surface fluxes composited from those simulated in REF. In these simulations, the radiation scheme is not activated, but the diurnal composite of the θ tendency from radiation (also computed from REF) is added to the large-scale advection. This simulation seeks to assess the role of surface–atmosphere interaction.

We also discuss the results of the SCM framework in comparison with a 2D meridional-vertical framework developed by Peyrillé and Lafore (2007) to study a typical monsoon regime. This 2D framework seeks to represent the first-order dynamics of a simplified West

African monsoon in an idealized configuration and has already been used to study the diurnal cycle in two contrasted areas (ITCZ versus arid Sahara desert). The comparison of the 2D and SCM approaches might give some insight into the significance of dynamical feedbacks for the diurnal cycle since the host model and the physical package are the same for both types of simulations.

3.4 Observations Used for Validation

Observations (radiosoundings, surface meteorological, radiative and turbulent flux measurements, ceilometers) collected during the AMMA field campaign are used to evaluate the model over the four different types. Those observations document the surface energy budget, thermodynamic and dynamic vertical structures and cloud characteristics.

More detailed documentation on cloud characteristics are available for the convective and semi-arid type, where the ground lidar and radar from the atmospheric radiation measurement mobile facility (deployed in Niamey) provide information on the vertical profiles of cloud fraction and occurrence as shown in Bouniol et al. (2012). In addition, vertical composite profiles derived from the spaceborne cloud radar and lidar on board Cloudsat and Calipso satellites (belonging to the A-Train constellation) averaged over a 10°W–10°E section for a month are used to assess qualitatively the expected cloud fraction for the four types.

Regarding the precipitation, ground observations (about 30 stations in the area of Niamey) have been used as well as satellite estimates: rainfall estimation version 2.0 data (RFE2, Love et al. 2004) with a resolution of 0.1 ° and 1 day and the Global Precipitation Climatology Project (GPCP, Huffman et al. 2001) with a resolution of 1 ° and 1 day.

4 Evaluation of the Modelling Framework

In this section, the REF simulations for the different types are evaluated. We only focus on the thermodynamical characteristics since the wind is controlled by nudging.

4.1 The Different Types: Reproducibility of Biases

As shown in Fig. 5a, the broad thermodynamical characteristics of the different types are reproduced by the modelling framework with in particular the correct stratification in temperature and a larger diurnal range of θ in the semi-arid type than in the convective wet type. These features were at least qualitatively simulated in the 2D modelling framework of Peyrillé and Lafore (2007) and further comparisons are presented in Sect. 4.6. For the two warmest cases, there is an important drying of the boundary layer during the day due to the large growth of the boundary layer that the model is able to reproduce (Fig. 5b). The important drying is linked to the large sensible heat flux and small evaporative fraction (as shown for example in a case study by Couvreux et al. 2012, see also Medeiros et al. 2005). This differs from the diurnal cycle observed by Betts et al. (1996) in the mid-latitudes (Kansas, grassland) in summer, which displayed an early morning moistening of the boundary layer with only small fluctuations of the water vapour mixing ratio during the remainder of the day, indicative of a balance between the entrainment and surface processes (Mahrt 1991). The model is able to reasonably represent the increase of boundary-layer height (h, determined by the level where $\theta > \theta_m + 0.2$ with θ_m the averaged virtual potential temperature of the lower levels) for warmer cases in relationship with a larger sensible heat flux and lower stability.

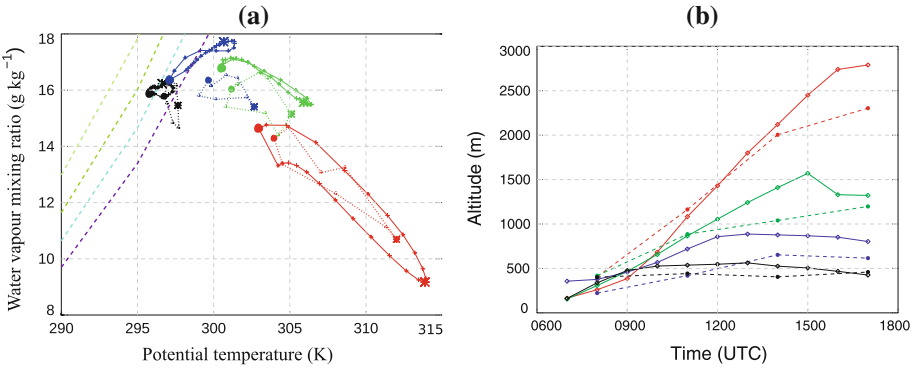

Fig. 5 **a** Diurnal cycle of r_v as a function of θ averaged in the first 500 m for the different types (same colour code as Fig. 2) from observations (*dotted lines*) and REF simulation (*full lines*). The *dashed lines* correspond to the saturation line for different pressure (950 hPa in *purple*, 970 hPa in *light blue*, 990 hPa in *dark green*, 1,015 hPa in *light green*). The averaged pressure of the first 500 m is about 990 hPa for cloudy and 960 hPa for convective wet. The *dots* corresponds to the values at 0600 and the stars at 1800 UTC. **b** Daytime evolution of the boundary-layer height for the different types in the observations (*dashed line*) and the REF simulations (*full line*)

But the model systematically overestimates h as shown in Fig. 5b except for the cloudy type (black line).

This modelling framework also reproduces some of the biases observed in NWP such as, (i) the poor representation of the diurnal cycle of the cloudy type with a underestimation (resp. overestimation) of the amplitude of the r_v (resp. θ) diurnal cycle, in relation with a state closer to saturation in the models than in the observations, and (ii) a cold bias for the convective wet type, linked to a too large impact of the convective scheme. The SCM also appears too moist for the convective type. This result is sensitive to the prescribed advection. Indeed, using the original advection derived from the AMMA re-analysis (without taking into account the small correction presented in Sect. 2.3b) leads to an underestimation of the occurrence of deep convection. The 10 % correction leads to a better prediction of the deep convection but also to a moist bias and a too synchronous θ and r_v diurnal cycle.

In the following, the vertical structures, the surface energy budget and the cloud characteristics for each type are analyzed in more detail.

4.2 Vertical Structures

Figure 6 presents observed and simulated mean vertical profiles for the four types focusing on the four synoptic hours 0600, 1200, 1800 and 0000 UTC. It illustrates the main differences in the representation of the diurnal cycle and also relates the vertical structures to the observed biases at low levels presented in Fig. 5a. Some differences already exist at 0600 UTC due to the model initiation with the ECMWF re-analysis instead of the soundings, but they generally remain small.

For the semi-arid type (Fig. 6a, b), at 1200 and 1800 UTC, the simulated boundary layer is too warm and too deep, consistently with Fig. 5b. The fine vertical structure and in particular the separation between the boundary layer and the Saharan air layer is not well simulated despite the use of high vertical resolution. Most of the days, the model predicts a boundary-layer height reaching the top of the Saharan air layer that also results in a too strong stratification at its top. The excessive growth of the ABL leads to an overestimation/underestimation

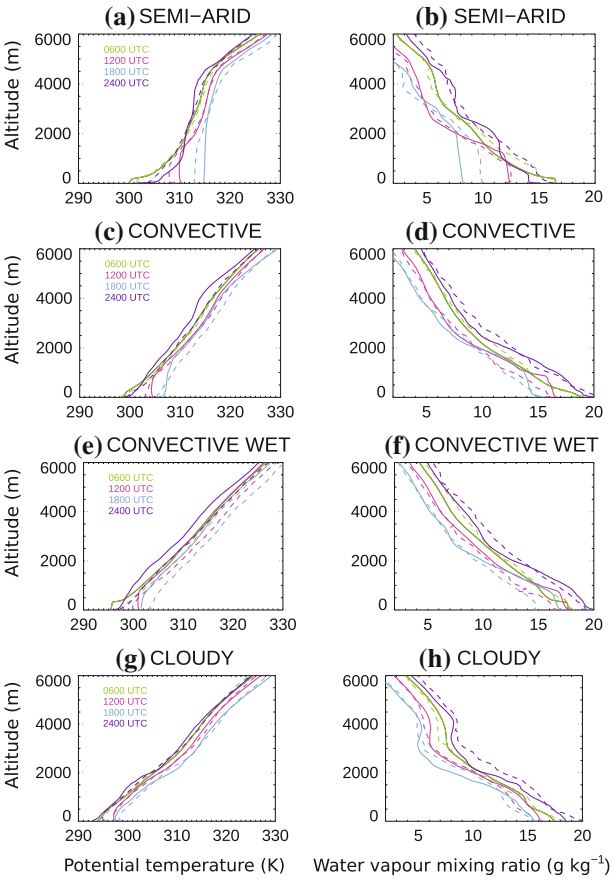

Fig. 6 Vertical profiles of θ (*left figures*) and r_v (*right figures*) of the diurnal composite for the semi-arid (**a**, **b**), the convective (**c**, **d**), the convective wet (**e**, **f**) and the cloudy types (**g**, **h**) in the models (*full line*) and in the observations (*dashed lines*). In order to make the profiles more visible, they have been offset by 1 K/+1 g kg^{-1} for the 0600 UTC profiles, +1 K/−1 g kg^{-1} for the 1800 UTC profiles and 2 K/+2 g kg^{-1} for the 0000 UTC profiles

of the ABL temperature/moisture during the course of the day. In contrast, the simulated nocturnal boundary layer is always too thin at 0000 UTC and the observed nighttime cooling extends over a much deeper layer. Explaining this difference is not straightforward and involves limitations in the land-surface and turbulent parametrizations, but possibly also involves an underestimation of the mixing by the nocturnal low-level jet (the winds being nudged towards a re-analysis characterized by lower winds, G12). In addition, at night the model underestimates the moistening at low levels, suggesting also an underestimation of the advection by the monsoon flow.

For the convective type (Fig. 6c), the model becomes too warm at mid-day and in the afternoon. The model reproduces to some extent the relatively stable and moist boundary layer observed at 1800 UTC following daytime deep convection. The boundary-layer height is still overestimated, especially at 1200 UTC, but to a lesser extent than for the semi-arid case. Similarly, the cooling at night occurs within too thin a layer.

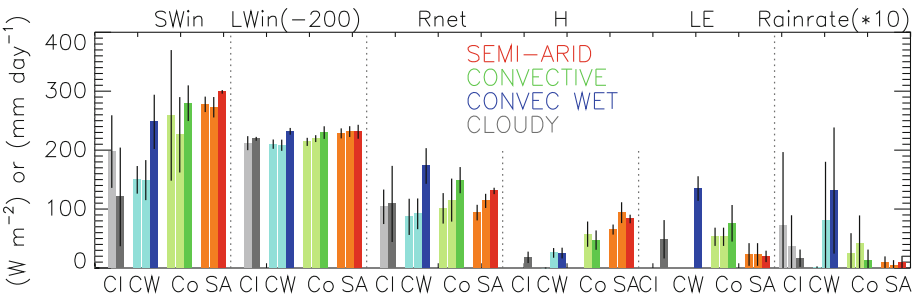

Fig. 7 Daily averages of different variables for the four different types ('Cl' for cloudy, 'CW' for convective wet, 'Co' for convective and 'SA' for semi- arid) in simulations (*dark colours*) and in observations (*light colours*): incoming short-wave radiation (*SWin*), incoming long-wave radiation (LW_{in} with a 200 W m^{-2} offset), net radiation (R_{net}), sensible heat flux (H), latent heat flux (LE) and rainrate (multiplied by ten). The *bars* materialize the synoptic variability among the different days (the average + or − the standard deviation are drawn). For each type, different sources of observations are used: the Impetus data for the convective wet and cloudy types, the AMMA catch for the convective wet type, the ARM Mobile Facility and the CEH data for the convective and semi-arid types

For the convective wet type, the model also produces a too deep convective boundary layer (Fig. 5b). At night, the cooling affects a thin or a deep layer, depending on the date, which is in agreement with observations even though the exact time sequence is not precisely reproduced (not shown). On the other hand, the low levels are now too cold (after mid-day) and moist (Fig. 6e, f) instead of too warm and dry in the former cases.

For the cloudy type, the simulated profiles of θ are closer to observations. Note however that the model tends to generate a stable nighttime layer at about 1800 m capped with cloud deck, which is not observed. Such an inversion is observed, but for r_v, and slightly higher (2,200 m). In contrast with the other cases, below 500 m, the amplitude of the diurnal cycle of r_v (Fig. 6h) is underestimated as shown also in Fig. 5a with too moist profiles during the day and too dry profiles during the night.

To summarize, for the two warmest types, the boundary-layer growth is excessive and the stratification at night occurs over too thin a layer leading to an overestimation of the amplitude of the diurnal cycle of θ. A cold bias characterizes the convective wet case and too small an amplitude of the r_v diurnal cycle for the cloudy type. In conclusion, distinct errors are found for the four cases showing that the drawbacks are type-dependent.

4.3 Surface Energy Budgets

In this section, the representation of the surface energy budget is analyzed, since boundary-layer behaviour is strongly framed by the surface fluxes and therefore the given surface energy budget. Figure 7 presents the daily averages of radiative, turbulent fluxes and precipitation as a function of the cases for the REF simulation and observations. Overall, the model is able to represent the main characteristics of the different types such as the increase of incoming solar radiation with temperature. The model also correctly reproduces the partitioning of the net radiation into latent and sensible heat fluxes for the semi-arid and convective types. However, some biases are highlighted below.

The model overestimates the incoming shortwave radiation (SW_{in}) for all regimes except the cloudy regime with different causes. The model largely (by 90 W m^{-2}) overestimates SW_{in} for the convective wet type (also evident in Fig. 8) likely due to an underestimation of the amount of deep convective clouds. This induces a maximum of net radiation (R_{net}) for this

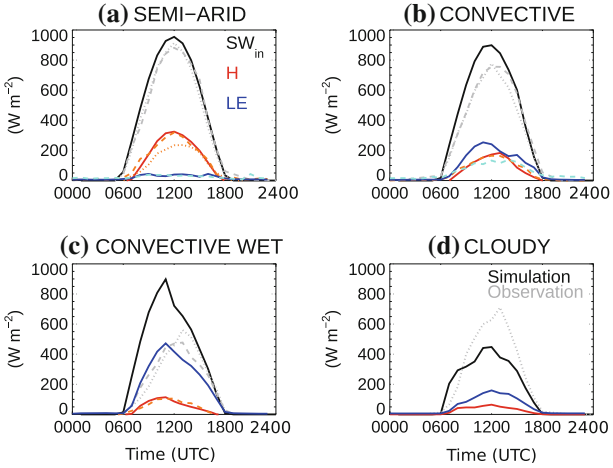

Fig. 8 Composite diurnal cycle of incoming shortwave radiation (*black* and *grey*), sensible heat flux (*red* and *orange*) and latent heat flux (*blue* and *cyan*) for the different types with simulations in *black*/*red*/*blue full lines* and observations in *grey*/*orange*/*cyan dot* or *dashed lines*. The *dashed line* corresponds to the ARM Mobile Facility flux measurements at Niamey for (**a**) and (**b**) and the measurements from Nalohou (AMMA-Catch) for (**c**). The *dotted line* corresponds to the measurement at Banizoumbou (from CEH) for (**a**) and (**b**) and from the Impetus network for (**c**) and (**d**)

type, which is not observed. G12 highlighted the almost constant R_{net} for the different types as opposed to the set of simulations, which displays a sharp maximum for the convective wet case. This has an impact on the surface energy partitioning between latent and sensible heat fluxes. If the sensible heat flux is in the range of observations, the latent heat flux is probably largely overestimated (as suggested by comparison to AMMA land-surface model intercomparison project, not shown). The overestimation of SW_{in} for the semi-arid type possibly involves the model climatological aerosol optical depth that is lower than observed (0.28 instead of 0.3–1). The low cloud fraction prevents any significant cloud radiative impact in this case (G12). As may be expected, the model does not represent well the day-to-day variability of SW_{in} for the semi-arid type since this variability (standard deviation of 15 W m^{-2}) is linked to synoptic fluctuations in aerosol concentration while, for simplicity, a fixed climatological aerosol concentration was used in the present simulations. The overestimation of the SW_{in} and R_{net} for the three warmest regimes is translated into an overestimation of the dominant flux for each regime, namely a slight overestimation of the sensible heat flux during the day for the semi-arid type (the latent heat flux is very low for this type) and an overestimation of the latent heat flux for the convective types (Figs. 7, 8). Note that, for the semi-arid regime, a large difference exists in the observational dataset of the sensible heat flux collected at two different sites (one at the Niamey airport, dashed line in Fig. 8, characterized by a lower albedo and larger sensible heat flux, and, the other in the shrublands, dotted line in Fig. 8, characterized by a higher albedo; this basically reflects the importance of the surface albedo for this case). For the cloudy type, the model presents too small a value, too large a synoptic variability as well as too small a diurnal range (not shown) of SW_{in} (Fig. 7). This is linked to the overestimated cloud cover as shown in the next subsection. Note that this error is compensated by errors in the upwelling longwave radiation leading to similar values of R_{net}. Note, however, that despite the large cloud-related errors, LW_{in} is about the same in the observations and the simulations for all cases. Furthermore, LW_{in} is almost constant

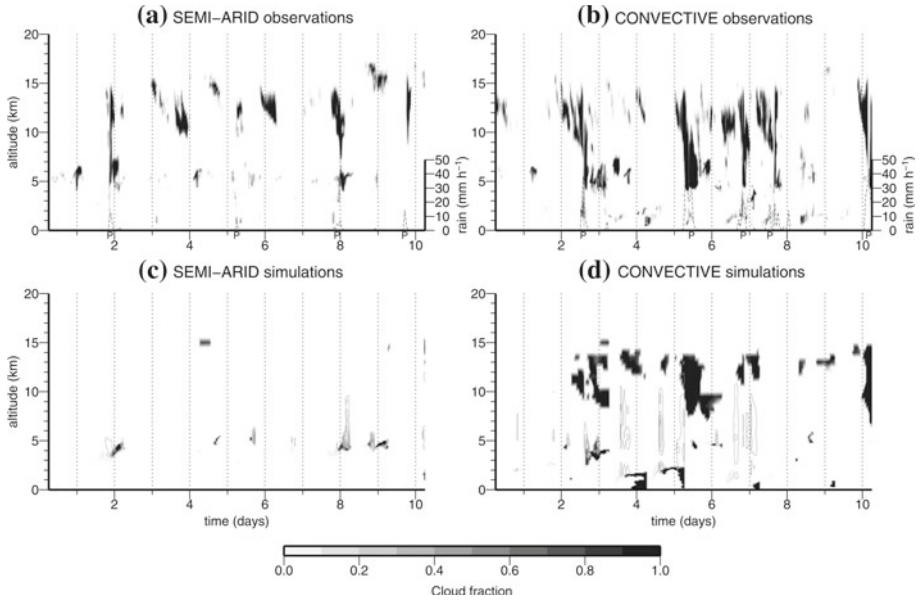

Fig. 9 Time series of the vertical profiles of cloud fraction simulated (**b**, **d**) and observed (**a**, **c**) at the ARM Mobile Facility for the semi-arid and convective types. In **a** and **c**, observed precipitation by the ground network is also indicated in *dashed line* with *p* in the *x*-axis indicating start of precipitating events. In **c** and **d**, the convective tendency is also overplotted in contours

among the different sites besides the differences in the moisture profiles as discussed in G12 (see also Guichard et al. 2009). This particular feature involves compensations between the impact of atmospheric temperature and humidity on radiative processes, and it appears to be reasonably well simulated.

Overall, R_{net} is overestimated for all cases apart for the cloudy type, and the positive bias is the largest for the convective wet case. This overestimation of R_{net} largely results from errors in SW_{in}. Errors in the radiative impact of aerosols are likely candidates for the semi-arid case, but errors associated with the simulation of clouds appear to play an important role elsewhere.

4.4 Cloud Cover and Precipitation

Since the cloud effect is a good candidate to explain the SW_{in} bias, we evaluate the representation of clouds in the models for the semi-arid and convective types with respect to the dataset presented in Bouniol et al. (2012). Some insights on the representation of clouds for the other two types are also given even though less data are available for their characterization.

For the semi-arid case, during the 10-day period, there were four observed events of rain that are indicated by 'p' in Fig. 9a. Among them, two events (the first and the third) correspond to several convective cells initiated in the afternoon and concern about seven of 30 stations within a $1^\circ \times 1^\circ$ area. Those events are characterized by small amounts of precipitation (about 3 mm[1] for each event). The occurrence and intensity of those events are correctly predicted by the model (Fig. 9b) suggesting that they are embedded within synoptic disturbances captured

[1] Those amounts of precipitation are relatively small but note that from 20 to 30 June 2006 there was a large-scale subsidence over West Africa that inhibited convection as shown by Janicot et al. (2008).

Table 3 Observed from satellite (RFE2, Love et al. 2004; GPCP, Huffman et al. 2001) and ground network and simulated precipitation (mm) for each type

Type	Cloudy	Convective wet	Convective	Semi-arid
RFE2 observations	36	80	41	5
GPCP observations	73	56	25	9
Ground observations	–	–	45	5
REF simulation	**21**	**111**	**34**	**9**

by the ECMWF re-analysis. Nevertheless, for these two deep convective events, the model strongly underestimates the cloud fraction (Fig. 9a,b). For the two other events, rainfall was recorded by only one station. The simulation of such small convective events is challenging, and it is not surprising that their timing is not well reproduced. In addition to deep convective clouds, Bouniol et al. (2012) underlined the existence of two other types of clouds associated with this semi-arid case, namely cirrus clouds (at about 12 km altitude) and mid-level clouds (at about 6 km altitude) that are evident in Fig. 9a. As may be expected, the model strongly underestimates the presence of cirrus as those types of clouds are often formed away from the observed location and further advected into the domain, a process that is not explicitly taken into account here. In five of the 10 days, mid-level clouds are simulated at the top of the Saharan air layer around 5 km, but still less than observed and over a smaller depth. In conclusion, the model manages to represent relatively well larger convective systems and their associated rainfall, but underestimates the mid-level clouds and strongly underestimates the cirrus clouds. The shallow cloud fraction is small in observations and null in the simulations.

For the convective case, four events generated rainfall at more than seven stations. Those events bring larger quantities of rain (about 9–10 mm per event). The model predicts three of these events even though too early for two of them. Overall, the occurrence and strength of the simulated deep convection is strongly constrained by the large-scale advection. The cloud fraction is better predicted but still underestimated for all cloud types. The model predicts shallow clouds for only four days instead of seven days in the observations.

Concerning the convective wet type, the model better predicts the initiation of deep convection, which occurred in most of the days and reproduces also a dry sequence at the end of the period (not shown) but it overestimates the amount of precipitation (Table 3; Fig. 7).

For the cloudy type, the model simulates some cirrus clouds above 9,000 m every day (not shown). Rapidly, a shallow cloud deck, reaching an altitude of about 1500–2000 m, develops. At 1100 UTC, such cloud decks are present except for three days. During the night, the clouds get thicker. Satellite observations suggest a deeper layer of shallow clouds but this could be an artefact, due to the vertical resolution of those products. The importance of shallow clouds in southern West Africa has been recently highlighted by Knippertz et al. (2011). In contrast to the climate models evaluated in this former study, here the model tends to overpredict their occurrence. Schrage and Fink (2012) showed that the formation of those stratiform clouds is tied to the existence of the nocturnal low-level jet. In fact, our modelling framework does reproduce this jet despite a small underestimation. This and the fine vertical resolution could explain that those clouds are reproduced in our configuration.

Concerning the precipitation, the model reproduces the different cumulative amounts of precipitation for the 10-day period as the simulated rainfall always stays within the range of observational products for all types as well as the distinct amounts among the different types as shown in Table 3 and Fig. 7.

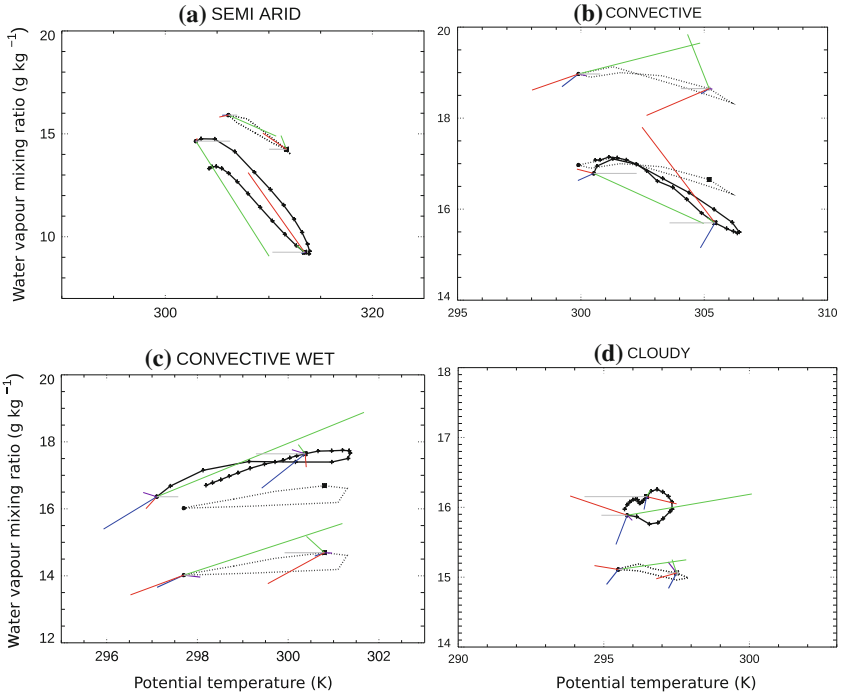

Fig. 10 Diurnal cycle of the low levels θ and r_v (*black lines*) with the rate of change of mixing ratio with potential temperature of each process: deep convection in *dark blue*, thermals and shallow convection in *green*, radiation in *grey*, microphysics in *purple* and large-scale forcing in *red*. The averaged daytime (0600–1800 UTC) rate of change of mixing ratio with potential temperature are plotted from the *dot* (0600 UTC point) whereas the averaged nighttime (1800–0600 UTC) one are plotted from an *asterisk sign* (1800 UTC point). The *black dashed line* corresponds to the diurnal cycle extracted from 2D simulation of Peyrillé and Lafore (2007) taking the point that has a similar mean potential temperature in the low levels. The averaged rate of change of mixing ratio with potential temperature from the same processes is also plotted. Note that, for convective and convective wet, the diurnal cycle with the tendencies overplotted are displaced by respectively +2 g kg^{-1}, −2 g kg^{-1} for clarity purpose

4.5 Balance Between Cloud, Radiative and Surface Processes

Figure 10 summarizes the diurnal cycles of the θ and r_v at low levels similar to Betts (1992); Freedman and Fitzjarrald (2001), and Santanello et al. (2009) with colour lines indicating the contribution of the different processes (plotted as a vector $[\Delta\theta,\ \Delta r_v]$ for a 12-h period considering separately daytime and nighttime) namely boundary layer in green (which includes turbulence and shallow convection), deep convection in dark blue, radiative processes in grey, large-scale advection in red and microphysics in purple. All the contributions correspond to the evolution of those variables provided by the different parametrizations except for the large-scale advection, which corresponds to the term prescribed in the simulation. For comparison with observations, the reader is referred to Fig. 5a. In addition, the composite of the diurnal cycle of SW_{in} is plotted for each case in Fig. 8.

In the semi-arid type, at night advection and radiation are predominant, whereas during the day, boundary-layer processes and radiation are active. This result is in line with Parker et al. (2005), Peyrillé and Lafore (2007), and Lothon et al. (2008) who find that the moisture

advected by the low-level jet during the night is then vertically redistributed by boundary-layer mixing during the day. The warming and drying biases discussed above account for the non-closed diurnal cycle.

The convective type involves similar processes with, in addition, a small cooling and drying induced by deep convective processes (namely convective downdrafts). The daytime evolution of θ and r_v is similar to the Santanello et al. (2009) results for summer in the southern Great Plains with non-cloudy processes dominating. Also, the change of the diurnal cycle in between semi-arid and convective types is linked to the difference in soil moisture content (cf. Table 1) as in this former study. Advection is much less important than in the semi-arid type in the low levels (below 500 m) analyzed here. It becomes more significant higher up (see Fig. 4). The relative magnitude of the cooling and moistening operated by advection also differs, i.e., the advected air is still cooler but somewhat less moist than in the semi-arid case. This is consistent with both a weaker monsoon flow and a reduced meridional gradient of r_v during the full monsoon. Note also that the too low cloud cover leads to a large overestimation of SW_{in} at the surface as discussed previously, besides a reasonable simulation of the magnitude of convective processes, especially in the morning during the growth of the boundary layer.

In the convective wet type, above the boundary layer, a commonly found equilibrium between vertical advection and deep convection is at play. Nevertheless, at low levels, boundary-layer turbulent mixing still dominate. A major difference with the previous cases is the moistening (instead of the drying) of the low levels by daytime turbulent mixing. For this case, while the convection scheme is very frequently activated and induces a non-negligible cooling and a drying of the low levels, the radiative impact of the associated clouds remains weak. Overall, the feedback of clouds on the surface energy budget, and therefore on the low levels, appears to be too weak, as shown in Fig. 7. In addition, the diurnal asymmetry (Fig. 8) is different with a more reduced SW_{in} in the morning in the observations (linked to the development of shallow clouds in the morning attested by the ceilometer, see G12 for more detail) compared to a larger reduction in the afternoon in the simulation. This suggests an underestimation of the shallow cloud cover.

The cloudy type, with the large cloud cover simulated at low levels, is characterized by a larger impact of radiative processes, especially at night. Contrary to the other types, they induce a cooling at both night and day. In fact, the very large simulated cloud cover likely accounts for the underestimation in SW_{in}. During the day, boundary-layer processes are balanced by advection, but also convective and radiative processes.

4.6 Comparing SCM Simulations with an Idealized Two-Dimensional Simulation

It is interesting to compare how these results stand with respect to those obtained with a more complex configuration of the model, involving interactions with the larger scales. The point here is to understand to what extent the diurnal-cycle characteristics are associated with the local physics and/or involve feedbacks with the dynamics. For this purpose, we compare the diurnal cycle obtained from an updated 2D simulation of Peyrillé and Lafore (2007). Here, the same model (MesoNH) with exactly the same physical parametrizations is used to explicitly simulate the large-scale atmospheric meridional circulation along a 2D latitude-altitude transect over West Africa during the monsoon. Such an idealized configuration is indeed able to reproduce major features of a mean summer monsoon from relatively simple surface and boundary conditions (Zheng and Eltahir 1998; Peyrillé et al. 2007). Note that as opposed to our simulations (through initial and boundary atmospheric conditions as well as soil conditions), information from observations cannot be directly incorporated in the

2D simulation. However, land-surface properties, sea-surface temperatures, and estimates of zonal advection are all inferred from observational datasets (see Peyrillé and Lafore 2007 for more detail).

In order to extract similar regimes from the 2D simulation, points with similar mean low-level potential temperature of the different cases have been extracted and are shown as dotted lines in Fig. 10. As expected since the large-scale meridional circulation is not constrained in the 2D model, the different cases exhibit differences, notably in humidity in regard to the SCM framework. The warmest type (semi-arid) is moister, and the convective wet and cloudy types are drier. However, the shape and magnitude of the diurnal cycles are surprisingly similar; apart from the semi-arid type. This suggests that the characteristics of the diurnal cycles for the different climates can be thought of as mainly driven by local processes. This point will also be addressed in more detail in the next section using sensitivity experiments. To go further, the contribution of the different processes is also compared. The different contributions are of same sign for the different types except for the convective type (Fig. 10b) for turbulent and advective processes, which tend to moisten the low levels in the 2D runs (similarly to the convective wet type, Fig. 10c) whereas there is drying at low levels in our framework. This difference might result from interactions between the meridional circulation and the local physics and this deserves further analysis. However, our simple SCM framework still appears quite valuable to analyze and improve basic aspects of the physical behaviour depicted by the model (with its parametrizations) over land under contrasted climates.

This section has demonstrated that this SCM framework allows us to reproduce many observed features of the various types encountered over land. The biases discussed above are tightly linked to the set of parametrizations of the model and are summarized in Fig. 11. They depend on the type (and convective regime) and develop rapidly within 24 h, revealing some complex and distinct interactions between processes. For the cloudy type, the model has difficulties handling the stratiform cloud layer, which is too prominent. This excessively reduces the SW_{in} at the surface and leads to a cold bias. For the convective wet and convective types, the cloud radiative impact is underestimated leading to a systematic overestimation of the SW_{in} and an overestimation of the latent heat flux. This leads to a moist bias. Finally, for the semi-arid type, the model has difficulties to handle fine structures and the convective boundary layer is too deep leading to a warm bias. The underestimation of cumulus cloud and aerosols also contributes to this bias.

5 Sensitivity Tests

In this section, we investigate how the set-up of the framework can be simplified without removing the main characteristics of the different types studied here. Therefore, we first analyze the impact of having a longer simulation instead of a one-day simulation and the role of diurnally varying advection. Eventually, the surface–atmosphere feedbacks are tackled by prescribing surface fluxes from the 1-day simulations.

5.1 1-Day Versus 10-Day Simulations

In this sub-section, we investigate the differences between long and short duration simulations. Instead of reinitializing the initial profiles every day as in REF, a single simulation is run over the 10-day period (referred to as COMPO simulation), using each day the same diurnal-varying composite large-scale advection shown in Fig. 4. For sake of simplicity, we only present simulations with a composite of the large-scale advection. However, simulations

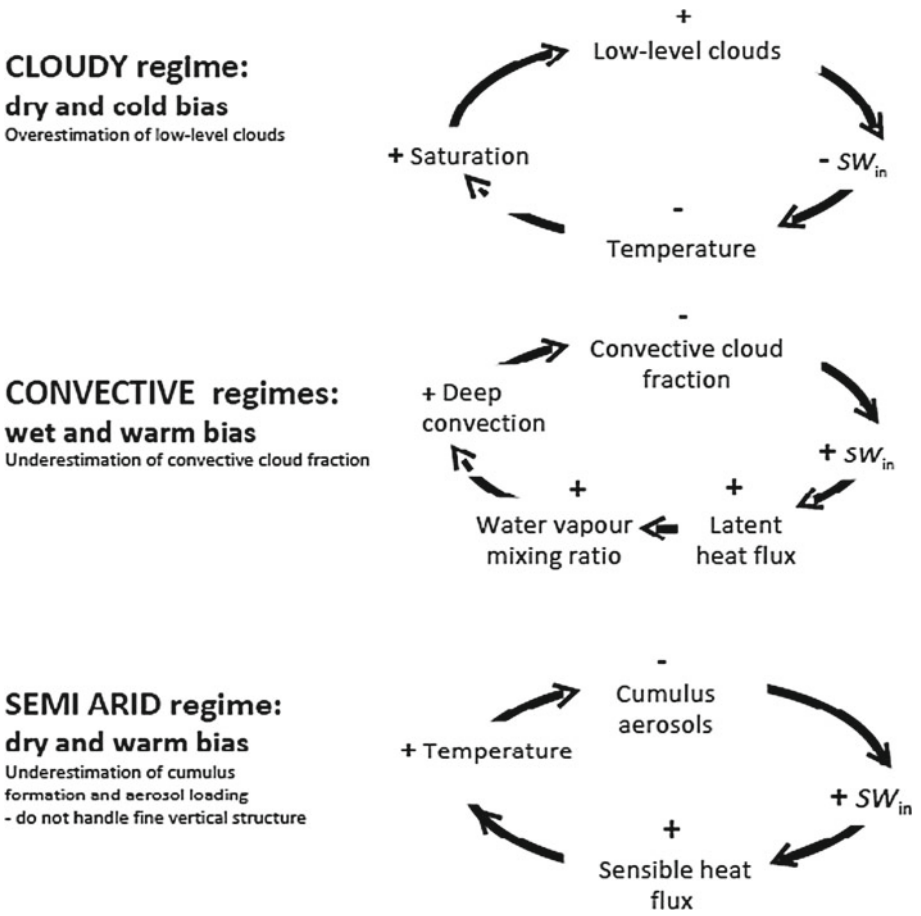

Fig. 11 Schematic of the different feedbacks at play depending on the type

with synoptically varying large-scale advection present the same behaviour as shown here, indicating that the differences between COMPO and REF are mainly related to the fact that simulations are longer and not to the synoptic fluctuations of advection. Here, we compare the COMPO simulations to the REF simulations for the four types.

In the semi-arid type, a warm and dry bias (Figs. 12, 13) develops rapidly below 3 km due to too large the growth of the boundary layer as already discussed for REF. This drift is not as pronounced in REF, because of the daily re-initialization, but it was identified by the non-closed diurnal cycle (Figs. 5a, 9a). In the COMPO simulation, equilibrium is reached after a few days, with a somewhat higher convective boundary layer than in REF (Fig. 14a). During the night, the cooling only affects a relatively thin stable boundary layer. Therefore, on the following day, this thin layer is eroded within a few hours, and after 0900/1000 UTC, the convective boundary layer quickly develops up to the same height every day. Such a development of the boundary layer has been observed but usually later in the day (Cuesta et al. 2009). This explains both the dry and warm bias and leads to a more pronounced and more humid residual layer top at about 5,000 m (Fig. 14a). This is also associated with the larger amount of mid-level clouds than in REF (Fig. 14c). These results suggest that

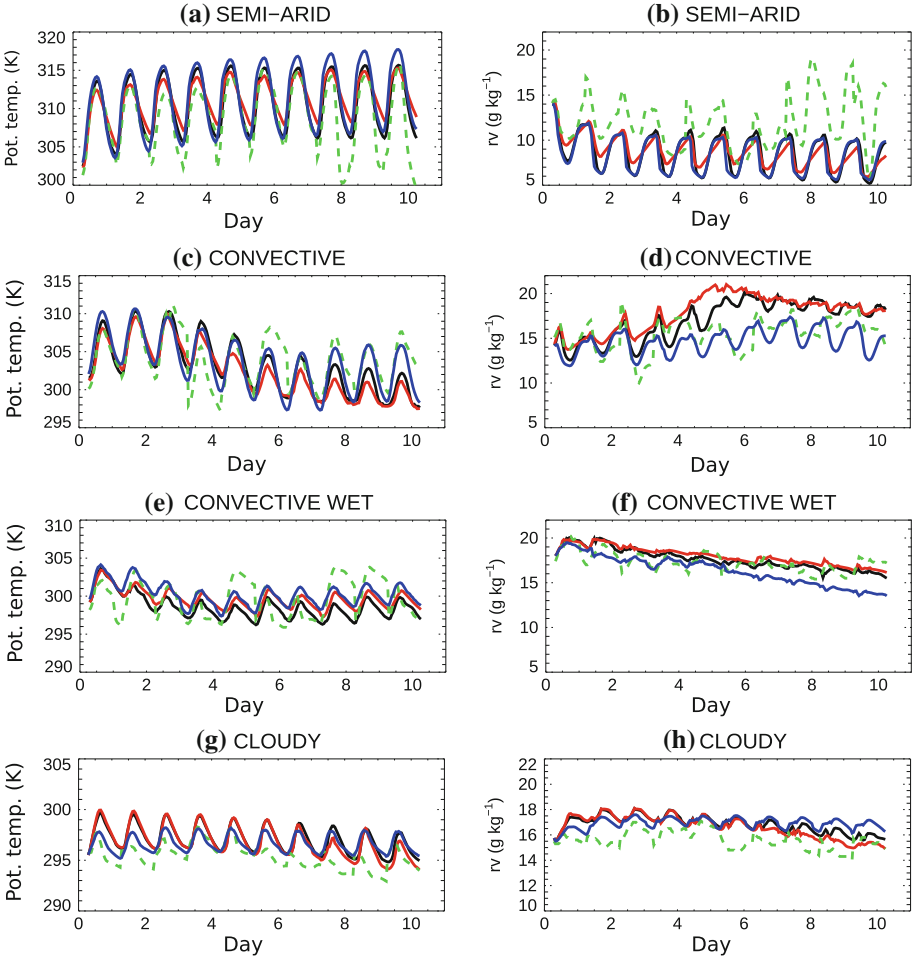

Fig. 12 Time evolution of the low-level (500 m) potential temperature (**a**, **c**, **e**, **g**) and water vapour mixing ratio (**b**, **d**, **f**, **h**) for the different types and the different simulations: REF in *green dashed line*, COMPO in *black*, CST in *red* and FLUX in *blue*

those mid-level clouds are strongly linked to the subtle vertical thermodynamical structure. Nevertheless, they have a much smaller impact on the shortwave radiation budget compared to observations (Bouniol et al. 2012).

In the convective type, the amplitude of the diurnal cycles of θ and r_v at low levels is similar to REF (Figs. 12, 13), but the low levels are slightly moister. Convection is more active, leading to more precipitation (46 mm) and to a larger cloud fraction (Fig. 14). Note also that, interestingly, convection is activated all along the 24 h instead of only during the afternoon in REF as shown in Fig. 15a with a maximum in the afternoon and during the night. This is related to the fact that the low levels which are never strongly stratified can quickly become well mixed up to about 5,000 m, leading more easily to deep convection triggering.

In the convective wet type, the low levels are colder than in REF (Fig. 13c), this corresponds to the signature of a few isolated days (Fig. 12e). Rain occurs every day in COMPO whereas it does not happen for three days in REF resulting in a higher cumulative amount of

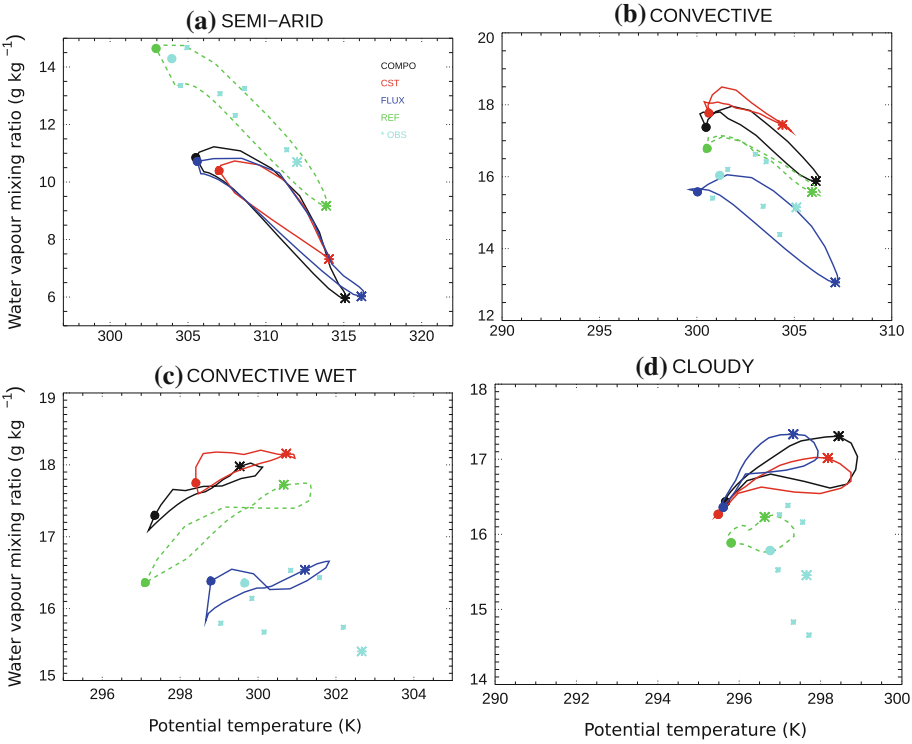

Fig. 13 Diurnal cycle of the low levels θ and r_v for the different types and the different simulations (*green dashed line* for REF, *black full line* for COMPO, *red full line* for CST, *blue full line* for FLUX and *cyan stars* for observations)

127 mm in COMPO (versus 111 mm in REF). COMPO displays higher values of soil moisture accompanied by larger latent heat fluxes and reduced sensible heat fluxes that prevent the boundary layer to warm as much during the day. The COMPO simulation predicts a too large cloud fraction in the upper levels (above 8,000 m) but strongly underestimates the occurrence of clouds in the lower levels as shown in Fig. 14i. The diurnal cycle of deep convection is also modified in COMPO compared to REF (Fig. 15b), with a 4 h earlier triggering of convection, shortcutting the shallow convection phase. Therefore, allowing longer-duration simulations induces substantial changes in the phasing of the diurnal cycle of deep convection that involves coupling with the surface-energy budget and the sensitivity of deep convective triggering to the atmospheric stability.

In the cloudy type, the COMPO simulation has a warm/moist bias compared to REF (Fig. 12), also consistent with the budget analysis. In this case, the diurnal cycle is partly framed by the saturation with a strong positive correlation between θ and r_v during the night, reflecting that r_v remains at saturation as θ decreases (Fig. 14). There is less cloud formation in the low levels with a strong diurnal cycle of shallow clouds (not shown) and precipitation increases to 34 mm (compared to 21 mm in REF).

In these simulations, most of the differences compared to the REF simulations are linked to the length of the simulation: longer simulation strengthens the biases already noticed in REF; e.g. the warm and dry bias for the semi-arid type and the moist bias for the cloudy type. For the convective wet case, part of the differences is also due to surface–atmosphere

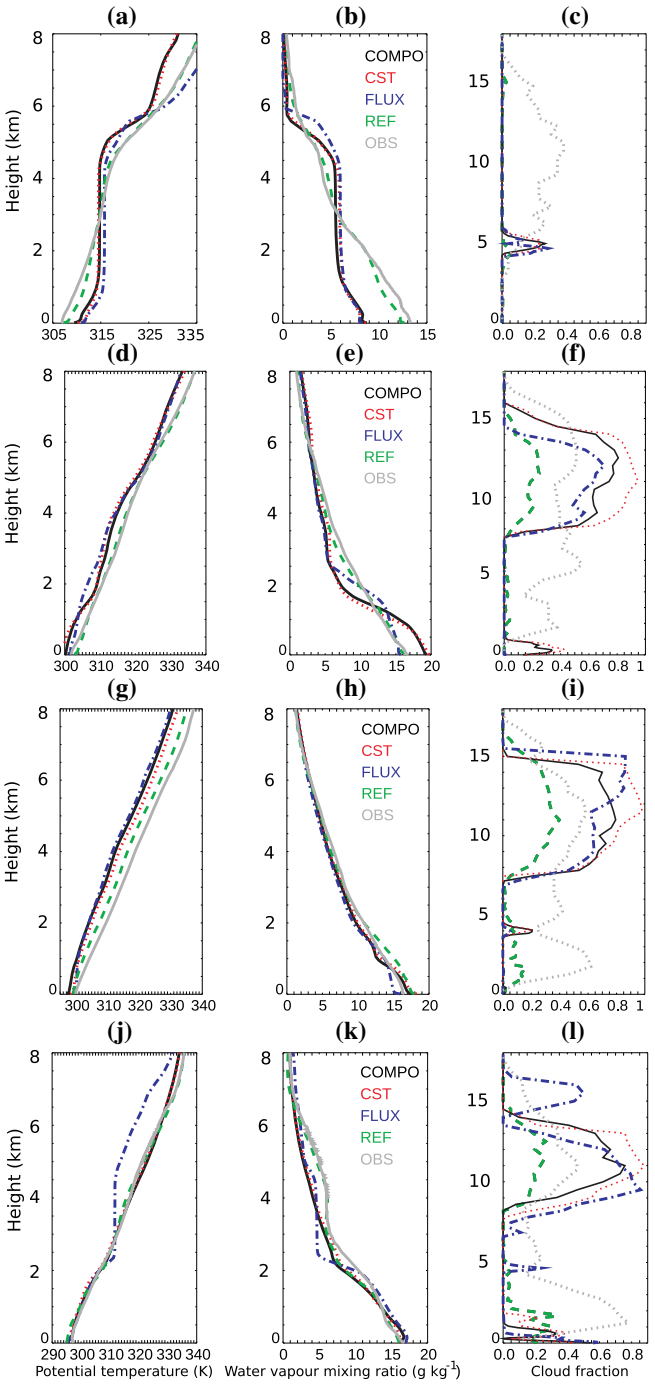

Fig. 14 Diurnally averaged vertical profiles for the last five days of θ, r_v and the cloud fraction for the different types. *Green dashed line* for REF, *black full line* for COMPO, *red dotted line* for CST, *blue dash-dot line* for FLUX and *grey line* for observations (θ and r_v profiles from radiosoundings and cloud fraction profiles derived from satellite)

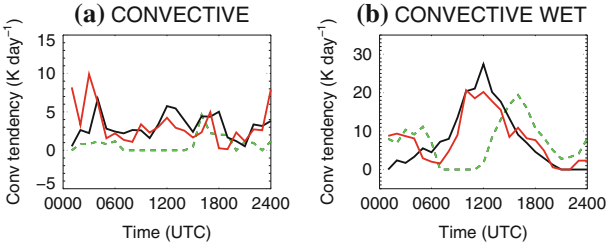

Fig. 15 Diurnal cycle of deep convection temperature tendency averaged in-between 4,000 and 12,000 m for the convective (in the *left figure*) and the convective wet (in the *right figure*) types. The *green dashed line* is the averaged diurnal cycle from the REF simulation, the *black line* is from COMPO simulation and the *red line* from CST simulation

feedbacks. It appears that several major features of the simulated 10-day period are already present in the series of 1-day simulations. This result emphasizes the quick thermodynamical drifts, which arise in the simulations during a few hours, especially during daytime.

5.2 Importance of the Diurnal Cycle of the Large-Scale Advection

In order to investigate the role of the large-scale advection diurnal cycle, 10-day long simulations with constant profiles of the large-scale advection (CST) have been performed. The synoptically varying large-scale advection controls the timing of deep convection in the semi-arid case or the pause of convective events in the convective wet case as illustrated in Sect. 4. Applying a diurnal composite of large-scale advection, without any synoptic variations, however, leads to relatively close mean diurnal cycles at low levels for the four types as shown in the previous section. Using constant (i.e. without any diurnal cycle) profiles of large-scale advection leads also to relatively small changes in the diurnal-averaged profiles as illustrated in Fig. 13. However, the amplitude of the diurnal cycle at low levels for the semi-arid and convective types is smaller by about 30 % in CST (Figs. 12, 13). This is consistent with Parker et al. (2005), who highlighted a strong diurnal cycle of the large-scale advection operated by the monsoon flow in the low levels. This is also evident in Fig. 10a,b, where the nighttime cooling and moistening is mostly driven by the advection. Figure 14 shows that in those simulations, the averaged cloud fractions are larger (except for the semi-arid type). A comparison of time–height budgets shows that there is no more erosion of the upper cloud layer in the morning by the large-scale advection. This suggests that the large-scale advection interacts with the cloud cover at sub-diurnal time scales. In agreement with Betts and Jakob (2002b), changing the phase of the large-scale advection did not lead to a strong modification of the diurnal case of deep convection, only the intensity of the different peaks varies as shown in Fig. 15. In the cloudy type, the differences are very small: they consist in a cold and dry bias in CST compared to COMPO (Fig. 13) due to the behaviour of the last days (Fig. 12), in particular the seventh day where in CST a very thick low-level cloud develops. This also explains the difference in the cloud fraction highlighted in Fig. 14.

In summary, the diurnal cycle of the large-scale advection partly drives the diurnal cycle for the semi-arid and convective cases, but it does not affect much the simulated diurnal cycle of both the low-level thermodynamics and rainfall for the convective wet type. In this latter case, the parametrized deep convection appears to respond more directly to surface and boundary-layer processes. These results confirm that the diurnal cycle in the low levels is

strongly controlled by processes operating at local scale rather than dictated by the large-scale dynamics as already pointed out by the similar behaviour of the SCM and 2D frameworks. On the other hand, the diurnal cycle of advection seems to at least partly shape and interact with the cloud cover in all cases (Fig. 14f, i, l).

5.3 Importance of the Land–Atmosphere Coupling

In order to test the impact of the land–atmosphere coupling, long simulations (FLUX) have been run with prescribed surface sensible and latent heat fluxes obtained from the composite diurnal cycle of the interactive fluxes resolved in the REF simulations. Compared to the COMPO simulations, the REF simulations generally display larger sensible heat fluxes (about 20 W m^{-2}, in average for the warmest cases, less for the other cases) and smaller latent heat fluxes (about 10 W m^{-2} reaching 40 for the convective case) for all types (not shown). In the FLUX simulations, the amplitude of the diurnal cycle is stronger for the warmer types namely the semi-arid and convective ones and weaker for the two coldest (convective wet and cloudy types) (Fig. 13) compared to the COMPO simulations.

In the semi-arid case, the boundary layer of the FLUX simulation is warmer and slightly higher than COMPO due to larger sensible heat fluxes. The top of the Saharan air layer has a stronger inversion explaining clouds over a thinner layer due to the stronger lid. However, the modifications of the clouds have no impact on the surface heat fluxes as they are prescribed. Even though the surface fluxes are the same as in REF, the FLUX simulation is drier and warmer. This is due to the long duration of the simulation as discussed in Sect. 5.1.

In the convective case, the boundary layer is drier and thicker in FLUX than COMPO due to the higher sensible heat fluxes. The bias observed in the moisture content at low levels of COMPO was probably due to the different surface fluxes as imposing fluxes from REF reduces it strongly (Fig. 12). The simulated clouds are similar except the shallow clouds that are absent in FLUX due to the higher lifting condensation level induced by the modification of the boundary-layer characteristics.

In the convective wet case, the boundary layer is also warmer and drier leading to a higher lifting condensation level and also no shallow clouds. In this simulation, the drift towards drier condition suggests that the model is not in equilibrium with the prescribed surface fluxes. For the cloudy type, the boundary layer is cooler from 1400 to 2300 UTC and this induces a weaker amplitude of the θ diurnal cycle than in COMPO, but the differences are relatively small. For this sensitivity test, most of the differences are explained by the differences in surface sensible and latent heat fluxes between COMPO and REF. However, parts of these differences are related to the cloud–land–atmosphere coupling: for example, we showed that the bias in the convective case was due to erroneous surface fluxes.

6 Conclusions

The diurnal cycle is a dominant mode of variability in the lower atmosphere over land in the Tropics. Operational models still have difficulties in representing the diurnal thermodynamics at low levels and their distinct fluctuations in time and location. This study, based on a large dataset collected over West Africa, used a single-column modelling framework that allows us to reproduce the synoptic forcing and enables us to evaluate the behaviour of a coupled surface–atmosphere model in different regimes encountered during summer over West Africa, from cooler to warmer conditions at low levels. A primary purpose of this multi-case approach is to allow for a more in-depth investigation of the interactions and

coupling between parametrized processes in a specific model. The modelling framework has been designed for single column models (SCM) or large-eddy simulation (LES) type models. Here, the SCM version of the Meso-NH model has been used, in a fully coupled mode with the surface scheme. Initial and boundary conditions have been designed from the AMMA re-analysis and ALMIP off-line runs. This is a rather simple modelling framework, which is however realistic enough to be able to capture the observed synoptic variability.

First, the modelling framework manages to roughly represent the different identified regimes along a meridional gradient and shows how different balances of processes arise from the colder to the warmer types. With this framework, we reproduce some of the biases of operational models and have investigated the causes. At short time scales (sub-diurnal and synoptic), important biases appear that are linked to an erroneous simulation of the surface–atmosphere–cloud coupling. In particular, the models always underestimate the cloud fraction, especially at low levels, except for the cloudiest case for which the low-level cloud cover is too large. Moreover, the cloud radiative forcing is largely underestimated in the simulations. This leads to an overestimation of the incoming shortwave radiation and therefore of the net radiation. How this bias translates into surface sensible and latent heat flux biases largely depends on the surface properties. Overall, this leads to dry and warm biases over relatively dry soil (semi-arid type) and cool and wet biases in wet soil conditions (convective wet type). Eventually, this study stresses the importance of the cloud radiative forcing over land, even for the drier cases: its representation needs to be accurate enough so as to avoid the rapid development of biases.

The interest of designing the framework from observed cases is to allow for an assessment of the performances of the model against observations. For further studies, a simpler framework appears as a valuable tool, in so far as it does not modify the basic properties of the simulated atmospheric low levels. This question was investigated with additional simulations, and it appears that simplifying the framework does indeed maintain the main biases as summarized below. Letting the simulations run for 10 days without daily reinitialization induces a modification of the diurnal cycle of convection, and then the drawbacks already visible in the one-day simulations are amplified. Imposing a constant-in-time advection induces a slightly reduced amplitude of the diurnal cycle for the two warmest types. This indicates that the diurnal cycle of the monsoon flow (which partly accounts for large-scale advection in these cases) plays a role in the observed diurnal cycle even if not a major one. In contrast, the diurnal cycle of large-scale advection has a very minor impact for the moistest types.

This study shows that the database presented in G12 is suitable to evaluate the behaviour of models regarding their simulation of the diurnal cycle displayed by the contrasted boundary-layer types observed in West Africa. We have also shown that our approach could be used to better understand the behaviour of more complex models such as the 2D monsoon model of Peyrillé and Lafore (2007). Indeed, at first order, the diurnal cycle at low levels displays similar behaviours in both SCM simulations presented here and 2D simulations using the same set of physical parametrizations.

This comparison of SCM and 2D frameworks has highlighted that the diurnal cycle mainly involves local processes with only limited feedbacks from the larger-scale circulations. In other words, errors in the simulation of the diurnal cycle of the boundary layer are related at first order to local processes, which involve physical parametrizations in the model. This provides evidence for the relevance of the relatively simple approach developed here. In the future, high-resolution simulations using the same set-up could be performed in order to further explore the processes and coupling mechanisms involved in the diurnal cycle and to assess the sources of biases arising in parametrized models.

Acknowledgments The authors are grateful to Rémi Cambra and Alexis Fradet who worked on this subject during their internship for a month and to Jean-Marcel Piriou for providing the ARPEGE runs. We thank Florence Favot for her everyday help and her capacity of always rapidly solving computer problems. The authors would like to thank the three anonymous reviewers for their careful comments. The authors are grateful to the AMMA International Program and to the whole dataset that was collected during this campaign. The Niamey AMF data were obtained from the Atmospheric Radiation Measurement (ARM) Program Archive of the Department of Energy.

References

Agusti-Panareda A, Vasiljevic D, Beljaars A, Bock O, Guichard F, Nuret M, Lafore JP, Mendez AG, Andersson E, Bechtold P, Fink A, Hersbach H, Ngamini JB, Parker D, Redelsperger JL, Tompkins A (2009) Radiosonde humidity bias correction over the West African region for the special AMMAreanalysis at ECMWF. Q J R Meteorol Soc 135:595–617

Agusti-Panareda A, Beljaars A, Ahlgrimm M, Balsamo G, Bock O, Forbes R, Ghelli A, Guichard F, Köhler M, Meynadier R, Morcrette JJ (2010) The ECMWF re-analysis for the AMMA observational campaign. Q J R Meteorol Soc 136:1457–1472

Bechtold P, Bazile E, Guichard F, Mascart P, Richard E (2001) A mass-flux convection scheme for regional and global models. Q J R Meteorol Soc 127:869–886

Bechtold P, Chaboureau JP, Beljaars A, Betts AK, Kohler M, Miller M, Redelsperger J-L (2004) The simulation of the diurnal cycle of convective precipitation over land in a global model. Q J R Meteorol Soc 130:3319–3337

Betts AK (1992) FIFE atmospheric boundary layer budget methods. J Geophys Res Atmos 97(D17):18523–18531

Betts AK, Jakob C (2002a) Evaluation of the diurnal cycle of precipitation, surface thermodynamics, and surface fluxes in the ECMWF model using LBAdata. J Geophys Res Atmos 107(D20):8045. doi:10.1029/2001JD000427

Betts AK, Jakob C (2002b) Study of diurnal cycle of convective precipitation over Amazonia using a single column model. J Geophys Res Atmos 107(D23):4732. doi:10.1029/2002JD002264

Boone A, de Rosnay P, Basalmo P, Beljaars A, Chopin F, Decharme B, Delire C, Ducharne A, Gascoin S, Grippa M, Guichard F, Gusev Y, Harris P, Jarlan L, Kergoat L, Mougin E, Nasonova O, Norgaard A, Orgeval T, Ottlé C, Poccard-Leclercq I, Polcher J, Sandholt I, Saux-Picart S, Taylor C, Xue Y (2009) The AMMA land surface model intercomparison project. Bull Am Meteorol Soc 90:1865–1880. doi:10.1175/2009BAMS2786.1

Betts AK, Ball JH, Beljaars AC, Miller MJ, Viterbo PA (1996) The land surface–atmosphere interaction: a review based on observational and global modelling perpective. J Geophys Res Atmos 101(D3):7209–7225. doi:10.1029/1995JD02135

Bouniol D, Couvreux F, Kamsu-Tamo PH, Leplay M, Guichard F, Favot F, O'Connor EJ (2012) Diurnal and seasonal cycles of cloud occurrences, types and radiative impact over West Africa. J Appl Meteorol 51:534–553. doi:10.1175/JAMC-D-11-051.1

Braam M, Vila-Guerau de Arellano J, Gorska M (2011) Boundary layer characteristics over homogeneous and heterogeneous surfaces simulated by MM5 and DALES. J Appl Meteorol 50:1372–1386

Couvreux F, Guichard F, Austin P, Chen F (2009) Nature of the mesoscale boundary layer height and water vapor variability observed 14 June 2002 during the IHOP_2002 campaign. Mon Weather Rev 137:414–432

Couvreux F, Rio C, Guichard F, Lothon M, Canut G, Bouniol D, Gounou A (2012) Initiation of daytime local convection in a semi-arid region analyzed with large-eddy simulations and AMMA observations. Q J R Meteorol Soc 138:56–71. doi:10.1002/aj.903

Cuesta J, Marsham J, Parker DJ, Flamant C (2009) Dynamical mechanims controlling the vertical redistribution of dust and the thermodynamic structure of the West Saharan atmospheric boundary layer during summer. Atmos Sci Lett 10:34–42

Cuxart J, Bougeault P, Redelsperger JL (2000) A turbulence scheme allowing for mesoscale and large-eddy simulations. Q J R Meteorol Soc 126:1–30

Dai A (2001) Global precipitation and thunderstorm frequencies. Part II: diurnal variations. J Clim 14(1112):1128

Dai A, Trenberth KE (2004) The diurnal cycle and its depiction in the community climate system model. J Clim 17:930–951

Del Genio AD, Wu J (2010) The role of entrainment in the diurnal cycle of continental convection. J Clim 23:2722–2738

Freedman JM, Fitzjarrald DR (2001) Postfrontal airmass modification. J Hydrometeorol 2:419–437
Gounou A, Guichard F, Couvreux F (2012) Observations of diurnal cycles over a West-African meridional transect: pre-monsoon and full-monsoon seasons. Boundary-Layer Meteorol 144:329–357. doi:10.1007/s10546-012-9723-8
Goutorbe JP, Noilhan J, Lacarrere P, Braud I (1997) Modelling of the atmospheric column over the central sites during HAPEX-Sahel. J Hydrol 188–189:1017–1039
Guichard F, Redelsperger JL, Lafore JP (2000) Cloud-resolving simulation of convective activity during TOGA–COARE, sensitivity to external sources of uncertainties. Q J R Meteorol Soc 126:3667–3695
Guichard F, Petch C, Redelsperger JL, Bechtold P, Chaboureau JP, Cheinet S, GrabowskiW Grenier H, Jones CG, Köhler M, Piriou JM, Tailleux R, Tomasini M (2004) Modelling the diurnal cycle of deep precipitating convection over land with cloud-resolving models and single-column models. Q J R Meteorol Soc 130:3139–3172
Guichard F, Kergoat L, Mougin E, Timouk F, Baup F, Hiernaux P, Lavenu F (2009) Surface thermodynamics and radiative budget in the Sahelian Gourma: seasonal and diurnal cycles. J Hydrol 375:161–177
Hastenrath S (1995) Climate dynamics of the tropics. Kluwer, New York 488 pp
Huffman GJ, Adler RF, Morrissey MM, Bolvin DT, Curtis S, Joyce R, McGavock B, Susskind J (2001) Global precipitation at one-degree daily resolution from multisatellite observations. J Hydrometeorol 2:36–50
Janicot S, Thorncroft CD, Ali A, Asencio N, Berry G, Bock O, Bourles B, Caniaux G, Chauvin F, Deme A, Kergoat L, Lafore JP, Lavaysse C, Lebel T, Marticorena B, Mounier F, Nedelec P, Redelsperger JL, Ravegnani F, Reeves CE, Roca R, de Rosnay P, Schlager H, Sultan B, Tomasini M, Ulanovsky A (2008) Large-scale overview of the summer monsoon over West Africa during the AMMA field experiment in 2006. Ann Geophys 26:2569–2595
Karbou F, Gérard E, Rabier F (2010) Global 4DVAR assimilation and forecast experiments using AMSU observations over land. Part I: impacts of various land surface emissivity parameterizations. Weather Forecast 25:5–19. doi:10.1175/2009WAF2222243.1
Knippertz P, Fink AH, Schuster R, Trentmann J, Schrage JJM, Yorke C (2011) Ultra-low clouds over the southern West African monsoon region. Geophys Res Lett 38:L21808. doi:10.1029/2011GL049278
Lafore JP, Stein J, Asencio N, Bougeault P, Ducrocq V, Duron J, Fischer C, Hreil P, Mascart P, Masson V, Pinty JP, Redelsperger JL, Richard E (1998) The meso-NH atmospheric simulation system. Part 1: adiabatic formulation and control simulations. Ann Geophys 16:90–109
Lothon M, Said F, Lohou F, Campistron B (2008) Observation of the diurnal cycle in the low troposphere of West Africa. Mon Weather Rev 136:3477–3500
Love TB, Kumar V, Xie P, Thiaw W (2004) A 20-year daily Africa precipitation cllimatology using satellite and gauge data. In: Proceedings of 14th conference on applied climatology, Seattle
Mahrt L (1991) Boundary-layer moisture regimes. Q J R Meteorol Soc 117:151–176
Masson V, Champeaux J-L, Chauvin F, Meriguet C, Lacaze R (2003) A global database of land surface parameters at 1 km resolution in meteorological and climate models. J Clim 16:1261–1282
Medeiros B, Hall A, Stevens B (2005) What controls the mean depth of the PBL? J Clim 18:3157–3172
Mlawer EJ, Taubman SJ, Brown PD, Iacono MJ, Clough SA (1997) Radiative transfer for inhomogeneous atmospheres: RRTM, a validated correlated-k model for the longwave. J Geophys Res Atmos 102(D14):16663–16682. doi:10.1029/97JD00237
Nesbitt SW, Zipser EJ (2003) The diurnal cycle of rainfall and convective intensity according to three years of TRMM measurements. J Clim 16(1456):1485
Nikulin G, Jones C, Giorgi F, Asrar G, Buchner M, Cerezo-Mota R, Christensen O, Dequé M, Fernandez J, Haensler A, van Meijgaard E, Samuelsson P, Sylla M, Sushama L (2012) Precipitation climatology in an ensemble of CORDEX-Africa regional climate simulations. J Clim 25:6057–6078. doi:10.1175/JCLI-D-11-00375.1
Noilhan J, Planton S (1989) A simple parameterization of land surface processes for meteorological models. Mon Weather Rev 117:336–349
Parker DJ, Burton RR, Diongue-Niang A, Ellis RJ, Felton M, Taylor CM, Thorncroft CD, Bessemoulin P, Tompkins AM (2005) The diurnal cycle of the West African monsoon circulation. Q J R Meteorol Soc 131:2839–2860
Parker DJ, Fink A, Janicot S, Ngamini JB, Douglas M, Afiesimama E, Agusti-Panareda A, Beljaars A, Dide F, Diedhiou A, Lebel T, Polcher J, Redelsperger JL, Thorncroft C, Wilson GA (2008) The AMMA radiosonde program and its implications for the future of atmospheric monitoring over Africa. Bull Am Meteorol Soc 89:1015–1027
Pergaud J, Masson V, Malardel S, Couvreux F (2009) A parameterization of dry thermals and shallow cumuli for mesoscale numerical weather prediction. Boundary-Layer Meteorol 132:83–106. doi:10.1007/s10546-009-9388-0

Peyrillé P, Lafore JP (2007) An idealized two-dimensional framework to study the West African monsoon. Part II: large-scale advection and the diurnal cycle. J Atmos Sci 64:2783–2803
Peyrillé P, Lafore JP, Redelsperger JL (2007) An idealized two-dimensional framework to study the West African monsoon. Part I: validation and key controlling factors. Atmos Sci 64:2765–2782
Pinty J-P, Jabouille P (1998) A mixed-phase cloud parameterization for use in mesoscale nonhydrostatic model: simulations of a squall line and of orographic precipitations. In: Proceedings of conference on cloud physics, Everett, WA, USA. American Meteorological Society, Washington DC, pp 217–220
Redelsperger JL, Thorncroft C, Diedhiou A, Lebel T, Parker DJ, Polcher J (2006) African monsoon multidisciplinary analysis (AMMA): an international research project and field campaign. Bull Am Meteorol Soc 87:1739–1746
Rio C, Hourdin F, Grandpeix JY, Lafore JP (2009) Shifting the diurnal cycle of parameterized convection. Geophys Res Let 36:L0780
Rio C, Grandpeix J-Y, Hourdin F, Guichard F, Couvreux F, Lafore J-P, Fridlind A, Mrowiec A, Roehrig R, Rochetin N, Lefebvre M-P, Idelkadi A (2013) Control of deep convection by sub-cloud lifting processes: the ALP closure in the LMDZ5B general circulation model. Clim Dyn 40:2271–2292
Roehrig R, Bouniol D, Guichard F, Hourdin F, Redelsperger JL (2013) The present and future of the West African monsoon: a process-oriented assessment of CMIP5 simulations along the AMMA transect. J Clim. doi:10.1175/JCLI-D-12-00505.1
Santanello JA, Friedl MA, Ek MB (2007) Convective planetary boundary layer interactions with the land surface at diurnal time scales: diagnostics and feedbacks. J Hydrometeorol 8:1082–1097
Santanello JA, Peters-Lidard CD, Kumar SV, Alonge C, Tao WK (2009) A modeling and observational framework for diagnosing local land–atmosphere coupling on diurnal time scales. J Hydrometeorol 10:577–599
Schlemmer L, Hohenegger C, Schmidli J, Bretherton CS, Schar C (2011) An idealized cloud-resolving framework for the study of midlatitiude diurnal convection over land. J Atmos Sci 68:1041–1057
Schrage JM, Fink AH (2012) Nocturnal continental low-level stratus over Tropical west Africa: observations and possible mechanisms controlling its onset. Mon Weather Rev 140:1794–1809
Stratton RA, Stirling AJ (2012) Improving the diurnal cycle of convection in GCMs. Q J R Meteorol Soc. doi:10.1002/qj.991
Svensson G, Holtslag AAM, Kumar V, Mauritsen T, Steeneveld GJ, Angevine WM, Bazile E, Beljaars A, de Bruijn EIF, Cheng A, Conangla L, Cuxart J, Ek M, Falk MJ, Freedman F, Kitagawa H, Larson VE, Lock A, Mailhot J, Masson V, Park S, Pleim J, Söderberg S, Weng W, Zampieri M (2011) Evaluation of the diurnal cycle in the atmospheric boundary layer over land as represented by a variety of singlecolumn models: the second GABLS experiment. Boundary-Layer Meteorol 140:177–206. doi:10.1007/s10546-011-9611-7
Tegen I, Hollrig P, Chin M, Fung I, Jacob D, Penner J (1997) Contribution of different aerosol species to the global aerosol extinction optical thickness: estimates from model results. J Geophys Res Atmos 102(D20):23895–23915
Van Heerwaarden CC, Vila-Guerau de Arellano J, Gounou A, Guichard F, Couvreux F (2010) Understanding the daily cycle of surface evapotranspiration: a new method to quantify the influence of forcings and feedbacks. J Hydrometeorol. doi:10.1175/2010JHM1272.1
Yang CY, Slingo J (2001) The diurnal cycle in the tropics. Mon Weather Rev 129:784–801
Zheng X, Eltahir EAB (1998) The role of vegetation in the dynamics of West African monsoons. J Clim 11:2078–2096